전 용 필 교수 지도

석사학위 청구논문

Evaluating the Implantation of Trophoblast Cells in an Artificial 3D Uterine Model

2024

성신여자대학교 대학원

생물학과

김 지 선

Evaluating the Implantation of Trophoblast Cells in an Artificial 3D Uterine Model

Adviser: Yong-Pil Cheon, Ph.D.

Submitted in partical fulfillment
of the requirements for the degree of master.

Nov, 2023

Department of Biology

The Graduate School of Sungshin University

Ji Sun Kim

This is to certify that we have examined the
Master's Thesis of
Ji Sun Kim
Submitted to Department of Biology

Approved as to style and content:

Thesis Advisor .....

Committee Chairman .....

Committee Member .....

The Graduate School of Sungshin University

ABSTRACT

Evaluating the Implantation of Trophoblast Cells in an Artificial 3D Uterine Model

Ji Sun Kim
Department of Biology
Graduate School
Sungshin University

During early embryo development, implantation is a critical point for delivery rates in mammals. Besides, the high rate of implantation failure remains a major problem in artificial reproductive fields. However, the mechanisms of implantation failure are still poorly understood. Implantation is complex process that involves a delicate coordination and a dialog between the blastocyst and the endometrium. Implantation process in human is different in some degree from that of mice and rats, and limiting the application of findings from animal studies to humans. On the other hand, in vivo research on implantation in humans is constrained by ethical issues. So, for implantation research, it is necessary to establish a in vitro model similar to that of humans. In here, PEG hydrogel and epithelial cell line Ishikawa (receptive endometrium), AN3CA (non-

receptive endometrium) and human stromal cell line T-HESC were employed to mimic the endometrium, and choriocarcinoma cell lines (e.g. JAR JEG-3 and BeWo) for the blastocyst. The size of the spheroids increased with increasing culture time, and the cell viability was over 90%. The inner structure of the spheroids was full of cells, and Differentiated multinuclear cell structures were found at spheroid cultured for 72 h. In addition, different attachment and invasion rates were shown in response to epithelial cell monolayers of different properties. Through this, it can be seen that spheroids can grow and differentiate and have an appropriate reactivity to epithelial cells. Based on this, a 3D culture model was constructed. Put together, it is suggested that this configured model could be useful to mimic the maternal-embryo microenvironment and dissolve the various pathophysiological problems in human implantation.

CONTENTS

List of Tables

List of Figures

INTRODUCTION

Embryo implantation is a complex process that involves delicate coordination and interaction between the blastocyst and the receptive endometrium. In humans, at mid-secretory phase of the menstrual cycle, the uterus becomes "receptive" endometrium, commonly as a window of implantation (WOI) (Aghajanova et al., 2008). During WOI, the endometrium becomes receptive to implantation by estrogen and progesterone. Estrogen induces endometrial proliferation. As progesterone increases after ovulation, morphological and functional changes in the endometrium occur and promote a shift from the proliferative phase to the secretory phase. Meanwhile, the epithelial glands continue to grow, and the vasculature becomes a spiral; the endometrial thickness remains relatively constant, which leads to an increase in endometrial density (Chen et al., 2022). Under these conditions, the endometrium prepares for embryo implantation. During this period, embryo can implant and a competent blastocyst initiate attachment to the endometrial epithelial (Jason et al., 2021). The trophoblast proliferates and invades the decidualizing area (Carter et al., 2015).

Implantation consists of three processes: First, the blastocyst moves to the implantation site known as "pinopode" on the endometrium and forms a weak bond between the blastocyst and the endometrium (apposition). Second, trophoblast cells attach to the endometrium and form strong bonds (attachment). At this point, Integrin alpha V beta 3, known as the implantation marker, is expressed in both endometrium and blastocyst. Integrin is an adhesion molecule, and beta 3 is not expressed in human oocytes but has been reported to be expressed in syncytiotrophoblast. Third, trophoblast cells begin

to differentiate, they invade the endometrium stroma (invasion) (Rashid et al., 2011, Su-Mi Kim & Jong-Soo Kim, 2017, Hirota et al., 2019).

During the invasion process, the expression of MMP is increased, and MMP is associated with extra-cellular matrix remodeling by decomposing ECM protein (Gualdoni et al., 2022). Therefore, it is essential for the invasion and migration of cells, and the invasive capacity of the trophoblastic cell is related to the increase of MMP-2 and -9 (Staun et al., 2004). In addition, differentiation of the cytotrophoblast surrounding the blastocyst occurs. cytotrophoblast differentiates into syncytiotrophoblast and extravillous trophoblast (Silva et al., 2016). Syncytiotrophoblasts are formed by the fusion of villous cytotrophoblasts and cell fusion is a well-orchestrated process known to be mediated by syncytin-1 (ERVW-1) (Huang et al., 2013). The conversion from the mononucleated to the syncytial state results in alterations of the trophoblast phenotype over time, resulting in the production of placental hormones such as human chorionic gonadotropin (hCG) (Rothbauer et al., 2017). It also has the function of exchanging nutrients and gas into the placental barrier between the mother and fetal blood. On the other hand, extravillous trophoblast has an invasive property and invasion deep into myometrium (Velicky et al., 2016, Tarrade et al., 2001).

Embryo implantation is an important process in ontogenesis, and individual development is impossible without implantation. Pregnancy failure after assisted reproductive technology (ART) is 49.7%, and implantation failure is the main problem, so more research is needed to understand the implantation mechanism. For implantation research, it is necessary to establish an in vitro model similar to that of humans (Wang et al., 2012). Ethical problems exist in using human samples, and experimental animals such as mice have limitations

because they are different from the process of human implantation. Therefore, it is necessary to develop an in vitro model based on human cell lines.

The two-dimensional (2D) cell culture model was used to study the early fetal-maternal interaction. Primary epithelial and stromal cell monolayers mimicked the 2D endometrial environment, and trophoblast spheroids were used to mimic human blastocysts (Fitzgerald et al., 2021). This model enables us to investigate molecular events beyond the luminal epithelium-embryo attachment and endometrium dysfunction during reproductive failure. However, one of the main disadvantages of the 2D culture of primary endometrial cells is their reduced biological activities after several passages and diminished responses towards sex hormones, which are not supportive of studying their morphological and functional roles. So endometrial adenocarcinoma and immortalized epithelial cell lines began to be used (Hannan et al, 2010).

In addition, to overcome the limitation of 2D culture three-dimensional architecture have been employed. Among the culture plates used to develop 3D models, Transwell-type membrane cultures are widely used, as they foster a well-polarized and well-differentiated epithelial layer that communicates with stroma plated on the underside of the semi-permeable membrane or on the bottom of the culture dish (Pierro et al, 2001). While this approach allows the analysis of apical and basal compartments separately, it potentially distorts physiological interactions by physically separating cells and diluting paracrine signals (Cook et al., 2017).

Endometrial cell-extracellular matrix (ECM), a tridimensional (3D) matrix scaffold, provides biochemical and biophysical support to the endometrial cells. Monolayer culture without ECM alters the activity and secretion function of the endometrial epithelium (Jensen et al., 2020). The advantage is that collagen and

matrigel present more attachment ligands as bioactive hydrogels than inert hydrogels such as alginate and agarose (Miao et al., 2018). Therefore, Matrigel consists of various factors, including collagen type IV, and laminin, entactin is commonly used, but it has distinct disadvantages. Because Matgel is a raw material extracted from Engelbreth–Holm–Swarm mouse sarcoma, potential risk of transmission of animal pathogens that infect macrophages and affect the immune systems. (Kim et al., 2022). Both culture plate and matrigel limitations can be overcome by using synthetic hydrogel synthetic hydrogel, encapsulating stromal cells in synthetic hydrogel ECM, and plating epithelial cells on top to better express normal in vivo tissue structures, and providing a more physiological 3D environment for the resulting stromal cells (Cook et al., 2017).

polyethylene glycol (PEG)-based hydrogels and gelatin hydrogels have most commonly been employed as chemical tools to recapitulate key aspects of the extracellular matrix (Félix Vélez et al., 2022). The advantages of PEG hydrogels are that they can control the mechanical properties of the gel, easily control the scaffold structure and chemical composition, and show high cell visibility when the cells are encapsulated in the gel. PEG hydrogels do not support cell adhesion due to their bio-inert properties. However, RGD, a cell binding domain derived from Fibronectin, can be used to increase cell adhesion. In addition, a crosslinker composed of metalloprotease (MMP)-cleasable peptide is used to synthesize hydrogels that can be broken down into MMPs, providing an environment in which cells can diffuse or migrate, similar to the invasion phase during the implantation process.

So, here, a 3D culture model system was designed: PEG hydrogel and epithelial cell line Ishikawa (receptive endometrium), AN3CA (non-receptive endometrium) and human stromal cell line T-HESC, matrix to mimic the

endometrium, and choriocarcinoma cell lines (e.g. JAR JEG-3 and BeWo) to mimic the blastocyst. This configured model is a 3D model that mimics the uterus. It distinguishes the characteristics of the spheroids by cell line, The implantation rate was different by the epithelial lines, and the expression profiles of implantation markers were different between them. Those data suggested that my model may be useful in vitro study for human implantation.

MATERIALS AND METHODS

Cell lines

The human choriocarcinoma cell lines (JAR, JEG-3, BEWO), human endometrial stromal cell (THESC), and human endometrial epithelial cells (AN3CA, Ishikawa) were used in these studies. All cell lines were obtained from the America Type Culture Collection (ATCC). JAR cells were cultured in RPMI1640 (Gibco, Cat#31800-022, New York, US) supplement with 10% FBS (Sigma, Cat#12003C, Burlington, US), 2 mM L-glutamine (Sigma Aldrich, Cat#G5763, Burlington, US), 100 U penicillin and 100 μg/ml streptomycin. JEG-3 cells were cultured in Dulbecco's Modified Eagle Medium (DMEM) high glucose (Gibco, Cat#12100-046, Burlington, US) supplement with 10% FBS, 1 mM sodium pyruvate (Sigma Aldrich, Cat#P5280, Burlington, US), 100 U penicillin and 100 μg/ml streptomycin. BEWO cells were cultred Dulbecco's Modified Eagle's Medium/Nutrient Mixture F-12 Ham (Sigma Aldrich, Cat#D2906, Burlington, US) supplement with 10% FBS, 2 mM L-glutamine, 100 U penicillin and 100 μg/ml streptomycin. AN3CA cells were cultured in DMEM high glucose supplement with 10% FBS, 1 mM sodium pyruvate, 100 U penicillin and 100 μg/ml streptomycin. Ishikawa cells were cultured in DMEM:F12 supplement with 10% FBS, 2 mM sodium pyruvate, 100 U penicillin and 100 μg/ml streptomycin. THESC cells were cultured in DMEM:F12 supplement with 10% FBS, 2 mM sodium pyruvate, 100 U penicillin and 100 μg/ml streptomycin. All cell lines were cultured at 37℃, 5% CO_2. Media were changed every second day.

Spheroid culture

Human choriocarcinoma cell spheroids were generated according to our previous protocol with slight modifications. (Evans et al., 2020) Methylcellulose (4000 centipoises, Sigma Aldrich, Cat#M0512, Burlington, US) at 1.5% (w/v) was dissolved in DMEM medium by stirring at room temperature for 90 min followed by stirring overnight at 4°C and subsequent centrifugation for 90 min at 3500 rpm to remove insoluble methylcellulose. Human choriocarcinoma cell (JAR, JEG-3, BEWO) monolayers were detached with 0.25% trypsin-1.0 mM EDTA. JAR, JEG-3 and BEWO cells were seeded at densities of 1.5×10^3 cells/well, 2.5×10^3 and 2.5×10^3 respectively in non-treated U-type 96-well with 20% methylcellulose/80% DMEM spheroid media. Culture medium was added up to 150 µl after 30 minutes incubation.

Spheroids viability assay

Live/dead viability/cytotoxicty kit (invitrogen, #L3224, Massachusetts, US). Double stain viability assasy with calcein and ethidium homodimer-1 (Eth-D) to assess the viability of spheroid. Spheroids were cultured for 24 h, 48 h, 72 h and dual labeled with a final concentration of 5 µM calcein AM and 20 µM ethidium homodimer-1. Spehroids were incubated 30 min at RT. The labeled spheroid were placed single concave slide and imaged on LSM700 confocal microscope (Carl Zeiss, Oberkochen, Germany). Laser optimized and image obtain with of the Z-stack software.

Histology and Immunoflorescence

The spheroids were fixed 4% paraformaldehyde for 2h, transferred 70% ethanol, then embedded in paraffin. For histology analysis, 4 µm section were

stained with Hematoxylin (Vector Laboratories, California, USA) and Eosin (Eosin-Y 0.5% solution, Merk). Immunofluorescence was performed after deparaffinization and boiling the sample slide with 10 mM sodium citrate buffer (pH 6.0) for antigen retrieval. Samples were incubated with 1% normal goat blocking serum in PBS for 1 h. Then samples were incubated with beta hCG primary antibody (Novus, #NBP2-54685, dilution 1:200) and E-cadherin antibody (Cell signaling, #14472, dilution 1:200) in 0.1% BSA in PBS for 2h at RT. After washed in PBST and PBS incubated with Alexa Fluor 488 conjugate anti rabbit secondary antibody (Cell signaling, #4412, dilution 1:1000) and Alexa Fluor 594 conjugate anti mouse secondary antibody (Cell signaling, #8890, dilution 1:1000) for 1h at RT. Then the samples were washed and incubated with DAPI (1:100) for 30 min at RT. Slides were washed and mounted. The florescence signal was imaged on LSM700 confocal microscope (Carl Zeiss).

Attachment assay

The Ishikawa cells or AN3CA cells were seeded at 5× 10^4 cells per well in 24-well plate. Spheroids with diameter of 100–200 μm were selected and 10 spheroids were added onto Ishikawa or AN3CA monolayer. co-culture was maintained for 24 h, 48 h at 37°C under 5% CO2. Co-culture media was used in a mixture of endometrial epithelial cell medium : trophoblast cell medium = 1:1 (i.e. RPMI1640/DMEM:F12 1:1 case of JAR-Ishikawa). Briefly, spheroids were PBS washing and then subjected shaking at 140 rpm for 10 min.

3D endometrial culture

3D emdometrial culture was using TrueGel3D Hydrogel Kit (Sigma Aldrich, Cat#TRUE1, Burlington, US). 1x10^5 THESC cells were suspended in 50 μl RGD degradable polymer and CD cell-degradable crosslinker mixture. Plate the

mixture in insert well with 8.0 μm Transparent PET Membrane (Falcon, #353097, Las Vegas, US). After incubate the mixture at 37℃ for 20 minutes, Add 100 μl culture medium. After one hour of incubation, remove medium and seeding $7x10^4$ epithelial cells. And add 200 μl culture medium in well.

Prior to cell culturein hydrogel, the cells were labelled with the fluorescent vital dye, PKH26 (Sigma Aldrich, Cat#PKH26GL, Burlington, US) and PKH67 (Sigma Aldrich, Cat#PKH67GL, Burlington, US) according to the manufacturer's instructions. Image acquisition using LSM700 confocal microscope with Z-stack software.

Total RNA extraction and cDNA synthesis

Total RNA was extracted using RNeasy micro kit (Qiagen, #74004, Germany) and determined using Nanodrop Spectrophotometer (ThermoFisher, Massachusetts, US). Briefly, reaction reagents are 34 μl total RNA, 10 μl MMLV 5X buffer, 1 μl oligo dT primer (0.5 μg/μl), 1 μl random primer (0.1 μg/μl), 2 μl dNTP mix (100 mM). Reaction mixture was incubated at 65℃ for 5 min, placed at RT for 5 min, and then added with 4.5 μl DTT (100 mM), 2 μl M-MLV Reverse Transcriptase (Promega, #M170B), 1 μl RNase block ribonu-clease inhibitor (40 U/ml). The mixture was incubated at 42℃ for 1 h and 70℃ for 15 min to terminate cDNA synthesis. and kept -20℃ before it used.

Real-time PCR analysis

For quantification of expression levels, transcripts of target genes were amplified using reverse transcript(RT)-PCR and the specific primers (Table 2). Quantification real time RT-PCR was performed using SYBR Premix Ex Taq™ (TaKaRa, #RR420, Japan) and AriaMx Real-time PCR System (Agilent, #G8830A,

US). Information of the thermal cycle are in Table 1. Each reaction was run in triplicate and consisted of 1 μl cDNA. Dissociation curves were run on all reactions to ensure amplification of a single product with the appropriate melting temperature. The fold change in gene expression was calculated using the ΔΔCt method with the housekeeping gene, ribosomal protein, *36B4*, as the internal control.

Image analysis

Measurements of spheroid size and live and dead area in viability assay were determined by average diameter measurements and ROI managers using ImageJ software (NIH, Bethesda, US).

Statistics

the student's t-test, one-way ANOVA and Tukey's multiple-comparison test was performed to ecaluate the statistical significance beteen control and experiment group. Results were presented as mean ± SEM, SD. Values of $P < 0.05$ were considered significant. one-way ANOVA and Tukey's multiple-comparison test were using IBM SPSS statistic.

Table 1. Real-time RT-PCR Thermal cycler schedule

Step		Temperature(℃)	Time	cycles
Hold		94	30 min	1
3 steps PCR	Denaturation	95	1 min	45
	Annealing	59	30 sec	
	Extension	72	1 min	
Dissociation	Denaturation	95	15 sec	1
	Annealing	60	30 sec	
	Extension	95	15 sec	
Hold		4	Indefinitely	1

Table 2. Primer sequences for quantitative real-time PCR

Gene	Symbol	NCBI gene reference		Primer sequence (5'-3')	Amplified length (bp)
Homo sapiens growth differentiation factor 15	***GDF15***	NM_004864.4	S AS	GGTGAATGGCTCTCAGATGCT GTGTTCGAATCTTCCCAGCTCT	210
Homo sapiens endogenous retrovirus group W member 1	***Syncytin-1 (ERVW-1)***	NM_014590.4	S AS	AATGCAGCGTCCCGGAAATA ATCTTGAACTCCACCCCCATCA	247
Homo sapiens heme oxygenase 1	***HO-1***	NM_002133.3	S AS	AGCATGCCCCAGGATTTGT CTCTCCTTGTTGCGCTCAATCT	191
Homo sapiens CD44	***CD44***	FJ216964.1	S AS	ACAATGGCCCAGATGGAGAAAG GTGGAGCTGAAGCATTGAAGCA	207
Homo sapiens laminin subunit alpha 3	***LAMA3***	NM_198129.4	S AS	TGAATGTCGGCCAGGAGTTAC CATCCACTGGGGTTTTCTTTGTC	219
Homo sapiens selectin L (SELL)	***L-selectin***	NM_000655.5	S AS	GATGACGCCTGCCACAAACTAA CAAAGGGTGAGTACAGTCCATGGT	213
Homo sapiens integrin subunit alpha V	***ITGAV***	NM_002210.5	S AS	GCTGTCGGAGATTTCAATGGTGA AGTTTGCCATCAGAGCCACGAT	248
Homo sapiens integrin subunit beta 3	***ITGB3***	NM_000212.3	S AS	CGGCCAGATGATTCGAAGAA ACAAATGCCCCGAAGCCAAT	194
Human chorionic gonadotropin (hcg) beta subunit	***hCG β***	J00117.1	S AS	CTCTCAGCTGTCAATGTGCACTCT GCGGATTGAGAAGCCTTTATTGTG	201
60S acidic ribosomal protein P0	***Rplp0 (36B4)***	NM_007475	S AS	CGACCTGGAAGTCCAACTACTTCCT GCACCTTATTGGCCAACAGCAT	303

Table 3. Antibody information

Antibody	Description	Cat #	Company
E-cadherin	Mouse monoclonal	#14472	Cell signaling
Chorionic Gonadotropin beta Chain (hCG beta)	Rabbit polyclonal	NBP254685	NOVUS
Anti-rabbit IgG (H+L), F(ab')2 Fragment (Alexa Fluor® 488 Conjugate)	Goat polyclonal	#4412	Cell signaling
Anti-mouse IgG (H+L), F(ab')2 Fragment (Alexa Fluor® 594 Conjugate)	Goat polyclonal	#8890	Cell signaling
GAPDH	Mouse monoclonal	sc-32233	Santacruz

RESULTS

Growth of Spheroids originated from JAR, JEG-3, BEWO

Spheroids from all cell lines significantly increased in size over time (Fig. 1A-C). For JAR spheroids, the size increased significantly to 144.1±12 μm, 155.2±21.5 μm, and 162.6 μm ± 10.3 μm, respectively, during 24, 48, and 72 h. Similarly, JEG-3 spheroids size significantly increased to 151.52±13 μm, 160.6±17.9 μm, and 179.9±7 μm for each time. BEWO spheroids also significantly increased in size to 147.6±12.7 μm, 152.6±11.5 μm and 165.6±12 μm for each hour. Spheroid cultured for 24 h show a similar size to blastocyst, and these results confirmed that spheroids show a time-dependent growth pattern.

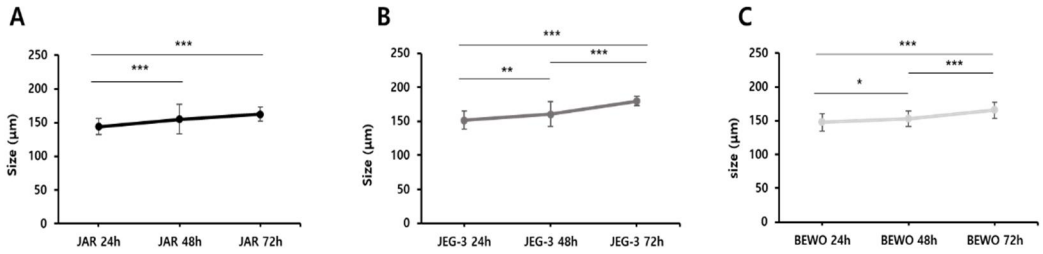

Figure 1. Changes in spheroid size over culture time

The size of the spheroid increased in a time-dependent. (A) JAR, (B) JEG-3, (C) BEWO. Data presented as mean ± s.d., n = 70. *Significant ($p < 0.05$); **Significant ($p < 0.01$); ***significant ($p < 0.001$).

Viability of the cells in Spheroids

The viability of cells constituting the spheroid was measured depending on the culture time. Calcein visualized live cells and ethidium homodimer-1 dead cells (Fig. 2). Analysis of z-stack images showed that more than 90% of cells survived during 24 to 72 hours of incubation. JAR spheroid showed 94±0.84%, 93±1.8%, and 94±1.61% cell viability, respectively, for 24 h, 48 h, and 72 h of culture time, and JEG-3 spheroid showed 96±1.15%, 95±0.11%, and 95±0.1%, respectively. BEWO spheroid showed 92±0.11%, 95±0.02%, and 94±0.93% cell viability during the 24 h, 48 h, 72 h, respectively, and there was no significant difference among cell lines.

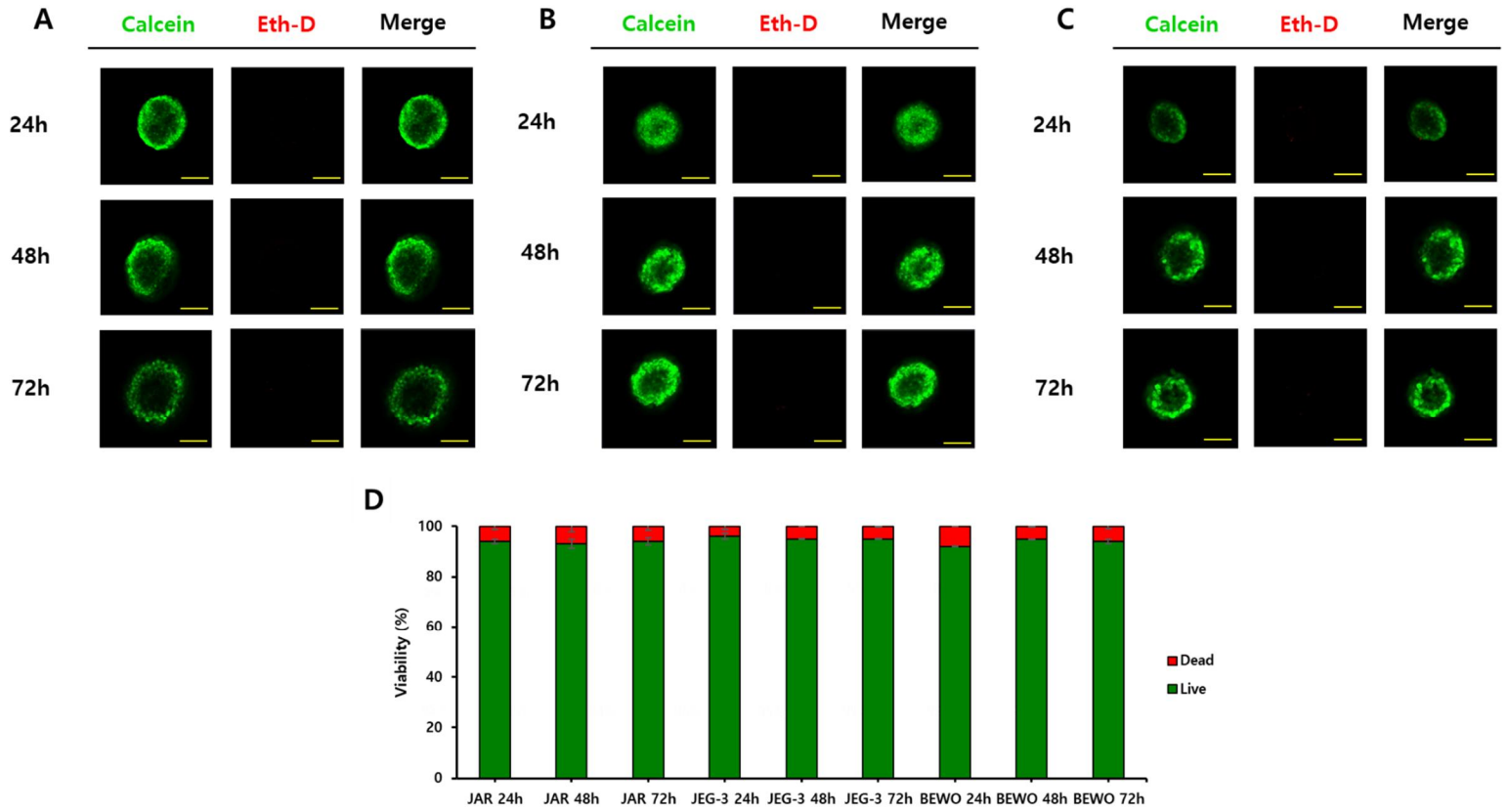
A
Calcein
Eth-D
Merge
24h
48h
72h
B
Calcein
Eth-D
Merge
24h
48h
72h
C
Calcein
Eth-D
Merge
24h
48h
72h
D
Viability (%)
100
80
60
40
20
0
JAR 24h
JAR 48h
JAR 72h
JEG-3 24h
JEG-3 48h
JEG-3 72h
BEWO 24h
BEWO 48h
BEWO 72h
Dead
Live

Figure 2. Viability of Spheroids

Z-stack image of spheroid. (A) JAR, (B) JEG-3, (C) BEWO, (D) The ratio of total live/dead cells percent. Spheroids growth with >90% live cells. Data presented as mean ± s.d., n = 3 spheroids; in each cell line. scale bars, 100 μm.

Histology of the cells in Spheroids

The internal structure of the spheroids was confirmed through histology analysis (Fig. 3). The inside of the spheroids was composed of intact cells, not empty structures. Spheroids cultured for 72 h showed differentiated cells of multinuclear structure (Fig. 3J).

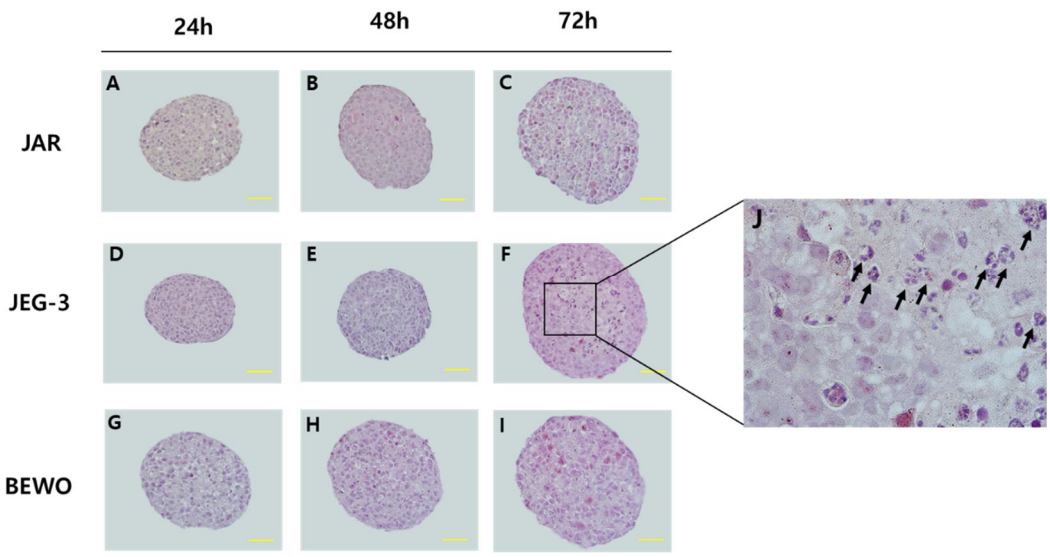

Figure 3. Histology of spheroid

H&E staining of spheroids. (A-C) JAR spheroid. (D-F) JEG-3 spheroid. (G-H) BEWO spheroid. (J) JEG-3 spheroid cultured for 72h magnification × 100. Differentiated cells of JEG-3 spheroid (arrow). scale bars, 50 μm.

Differentiation of trophoblast in the spheroid

Immunofluorescence was used to characterize the trophoblast cell type in spheroid. E-cadherin is present at intercellular junctions in human trophectoderm and mononuclear trophoblasts (Aplin et al., 2009), and was used to demarcate mononuclear cells. Spheroids formed by each cell line were hCG-positive starting from 24 hours of culture, and this positivity persisted up to 72 h. These results indicated that spheroids from each cell line comprised cytotrophoblasts and syncytiotrophoblasts (Fig. 4A).

β hCG fluorescence intensity increased significantly in all cell lines after 24 h. The BEWO spheroids cultured for 72 h showed the highest fluorescence intensity. However, there was no significant difference between each cell line (Fig. 4B). In addition, it was found that β hCG positive cells increased through the increase in the DAPI and β hCG ratio with the culture time (Fig. 4C).

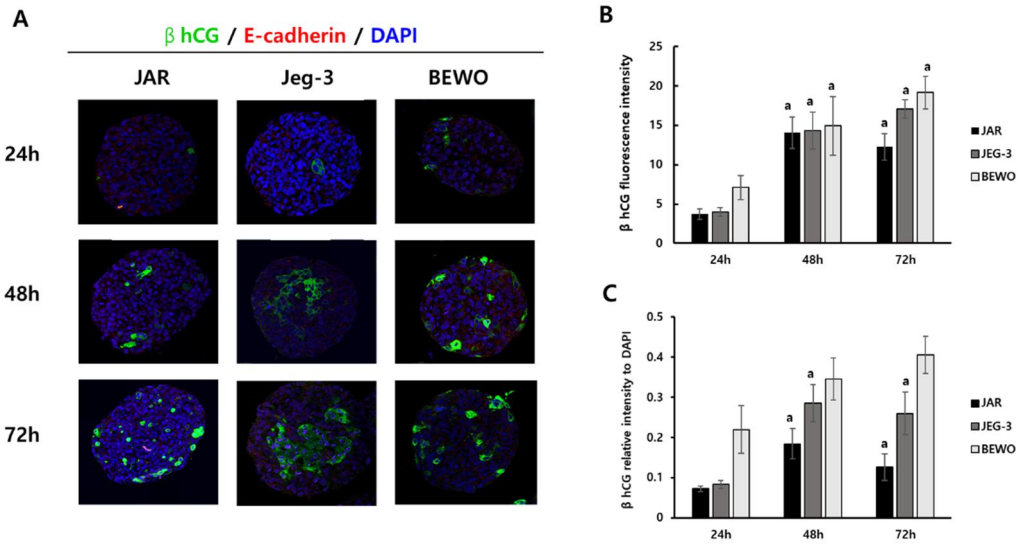

Figure 4. Syncytiotrophoblast marker expression in spheroids

(A) Spheroid performed immunofluorescence staining after incubation for 24,48 and 72 hours. The spheroids were β hCG positive at each culture time. The fluorescence image is a merge of E-cadherin (red), nuclear retaining (DPIA, blue) and β hCG (green). (B) quantification of the β hCG expression in spheroids. fluorescence intensities per pixel as means ± SEM. n = 5 spheroids; in each cell line. a: A significant difference between 24h.

Difference in implantation marker expressions.

Expression of implantation-related genes was examined to confirm the potential of spheroids for implantation processes. The expression of implantation markers of monolayer and spheroids by cell line was compared, respectively. The attachment or invasion markers CD44, L-selectin, LAMA3, integrin alpha V and HO-1 were not expressed in all cell line spheroids.

In all cell lines, the mRNA level of implantation-related genes was elevated when it was spheroids. The highest β hCG mRNA level was shown in the BEWO spheroid cultured for 72 h (Fig. 5A). Syncytin-1 is a gene that mediates cell

fusion, and it showed the highest level when cultured for 24 h in JAR and JEG-3 spheroid. BEWO spheroid continued to maintain elevated mRNA levels at 24 h (Fig. 5C). GDF15 is a gene that role in the migration and invasion of trophoblast cells (Zeng et al., 2023) and showed significantly higher mRNA levels in the JAR spheroid cultured for 24h (Fig. 5B). Integrin beta3 is a type of integrin, an adhesion molecule, and it showed high mRNA levels in 24 h spheroid, and BEWO spheroid remained high mRNA levels at 48 and 72 h (Fig. 5D).

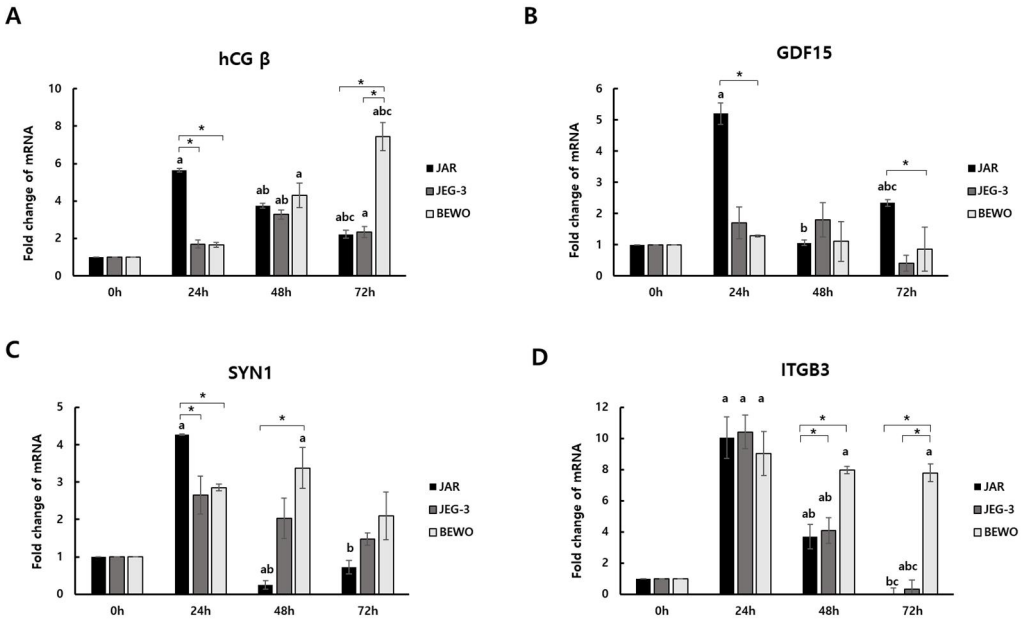

Figure 5. Expression levels of implantation markers

Gene expression was measured by RT-qPCR. Normalized to 36B4. (A) hCG β, (B) GDF15, (C) SYN1 (Syncytin-1), (D) ITGB3 (Integrin beta 3). *p < 0.05 (JAR vs JEG-3 vs BEWO). a: A significant difference between 24h. b: A significant difference between 48h. c: A significant difference between 72h.

Difference in attachment rate by the origin

The endometrial epithelial cell line, AN3CA (non-receptive) and Ishikawa (receptive) monolayer evaluated the attachment rate of spheroid for each cell line. After placing the spheroids on the endometrial epithelial cell monolayers, co-cultures were performed for 24 and 48 hours, resulting in different results depending on the characteristics of the monolayer.

In the AN3CA monolayer, JAR spheroid showed reduced attachment rates of 39.7% and 27.9%, respectively, at 24 h (n=63) and 48 h (n=68), but not significant. JEG-3 spheroid also showed reduced attachment rates to 54.6% and 42.6% at 24 h (n=75) and 48 h (n=54), respectively. BEWO spheroid showed an increased attachment rate over time, 73% and 82.5% at 24 h (n=52) and 48 h (n=40), respectively, and a significantly increased attachment rate compared to

JAR spheroid (Fig. 5A-F)

In Ishikawa monolayer, JAR spheroid showed 100% and 98% attachment rates at 24 h (n=72) and 48 h (n=50), respectively, and JEG-3 spheroid showed 97.5% and 93.3% attachment rates at 24 h (n=80) and 48 h (n=60), respectively. BEWO spheroid showed 100% and 98.3% attachment rates at 24 h (n=72) and 48 h (n=60). During Ishikawa and co-culture, all the cells showed high adhesion rates, and there was no significant difference between each cell line (Fig. 5G-M).

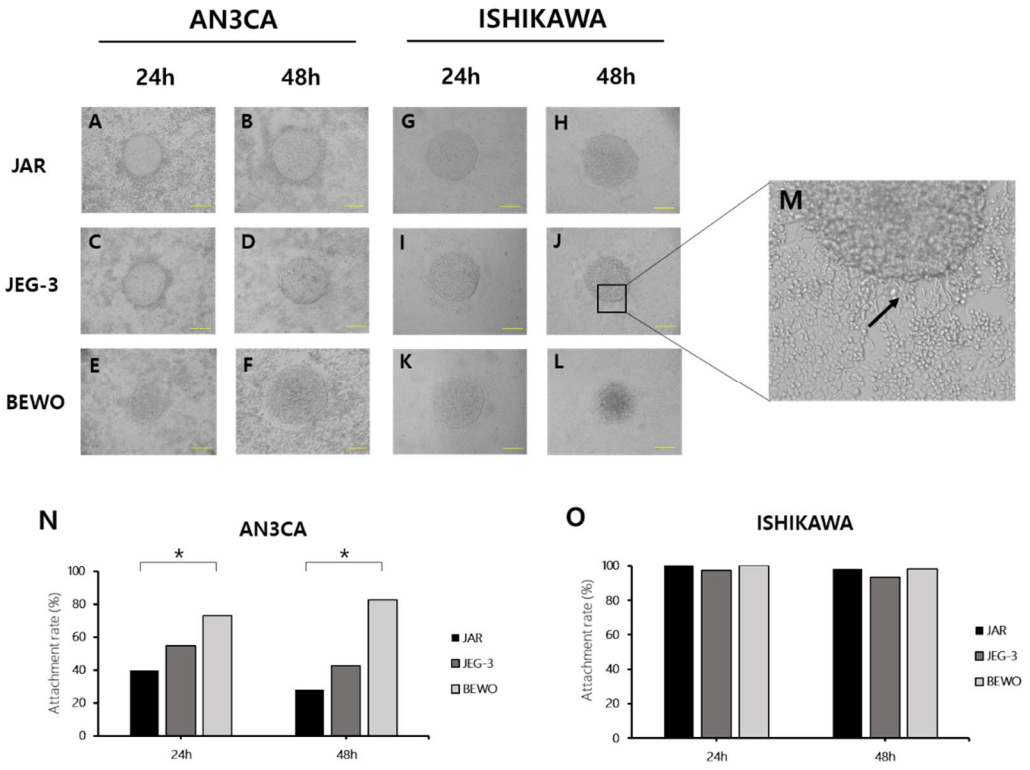

Figure 6. Attachment rates of spheroids

Attachment rate for each cell line. (A-F) Spheroid co-cultured with AN3CA monolayer (non-receptive) for 24h (JAR spheroids n=63, JEG-3 spheroids n=75, BEWO spheroids n=52), 48h (JAR spheroids n=68, JEG-3 spheroids n=54, BEWO spheroids n=40). (G-M) Spheroid co-cultured with Ishikawa monolayer (receptive) for 24h (JAR spheroids n=72, JEG-3 spheroids n=80, BEWO spheroids n=72), 48h (JAR spheroids n=50, JEG-3 spheroids n=60, BEWO spheroids n=60). (M) JEG-3 spheroid co-cultured with Ishikawa for 48 h. (arrow) branched spheroid cell. (N) attachment rate in AN3CA monolayer (non-receptive). (O) attachment rate in Ishikawa monolayer (receptive). scale bars, 50 μm. *Significant ($p < 0.05$).

Difference in invasion rate by the origin

At 48 h of coincubation with Ishikawa monolayer, the spheroid completely collapsed and migrated into the epithelial monolayer and invade (Fig. 7A). The proportion of invading spheroid among attached spheroid was measured after co-culture for 48 h. JAR spheoid showed invasion rates of 1.4% (1 out of 72). JEG-3 spheroid showed invasion rates of 12.5% (7 out of 56). BEWO spheroid showed invasion rates of 6.8 (4 out of 59). There was a significant difference in invasion rates between JAR spheroid and JEG-3 spheroid (Fig. 7B).

The invasion area of the collapsed spheroids was calculated. It was confirmed that the invasion area increased after 48 hours of co-culture (panel A yellow line). As a result, the JEG-3 spheroids showed the widest invasion area, followed by the BEWO spheroids. The invasion area of JEG-3 and BEWO spheroid was

significantly different (Fig. 7C).

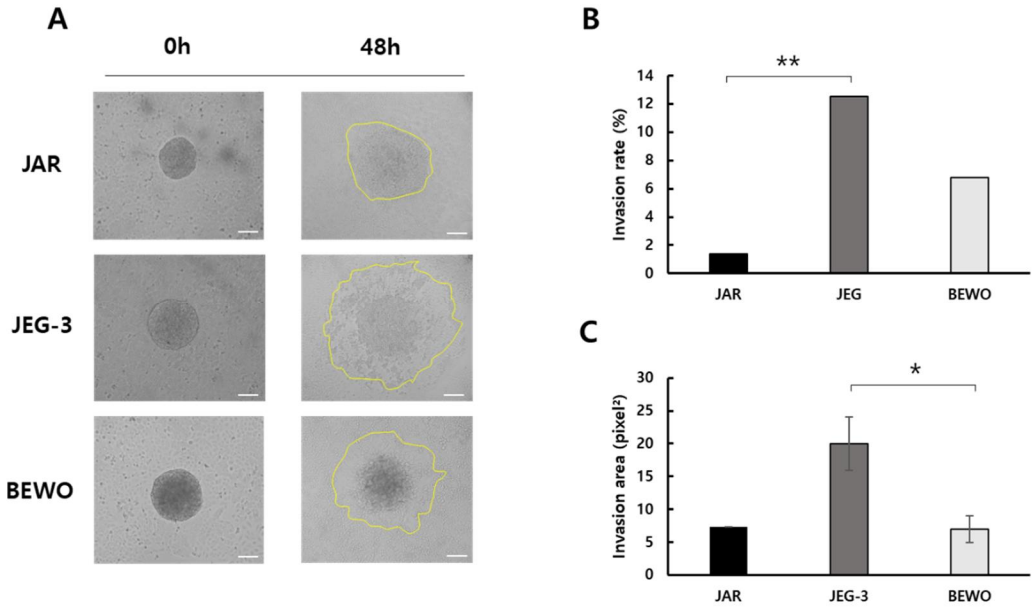

Figure 7. Invasion rates of spheroids

Invasion rate for each cell line. (A) Images after 48 hours of co-culture with Ishikawa for each cell line (JAR spheroids n=72, JEG-3 spheroids n=56, BEWO spheroids n=59). invasion areas are indicated by yellow lines. (B) invasion rate. (C) invasion area. This was quantified using image J. scale bars, 50 μm. Spheroid co-cultured with *Significant ($p < 0.05$); **Significant ($p < 0.01$).

3D culture models of human endometrium

A 3D culture system was established because there was a limit to research related to implantation with 2D culture. The diagram of 3D culture system construction, including the preparation of the matrix-stromal cells mixture and seeding of epithelial cells, and spheroids (Fig. 8A). After fluorescence labeling the stromal cell and epithelial cell, they were analyzed using a confocal microscope. the 3D culture system was confirmed by fluorescence microscopy (Fig. 8B). As a result, the stromal cell and epithelial cell compartments were well divided.

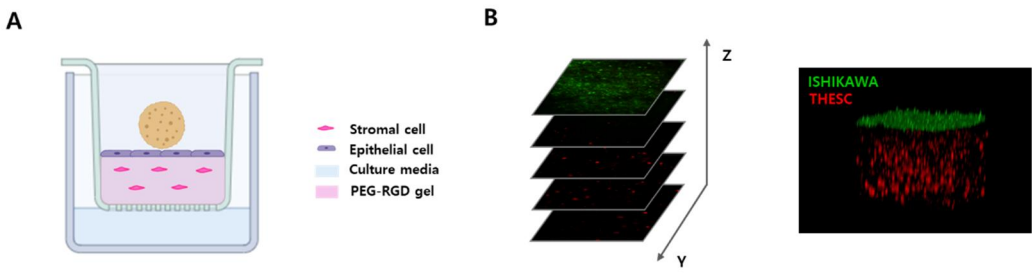

Figure 8. 3D culture models of human endometrium.

(A) Schematic diagram of the culture system. It is a structure in which stroma cells are encapsulated in the hydrogel in the insert well, and epithelial cells are placed on it. (B) culture day 6. Stromal cells were labeled PKH26 (red) and epithelial cells were labeled PKH67 (green).

DISCUSSION

In this study, spheroids were confirmed to be suitable for in vitro study through spheroid characterization. The spheroid size increased in a time-dependent manner, and the spheroids showed more than 90% viability. c and differentiated cells of the multinuclear structure were found at 72 h of culture (Fig. 1-3). These results suggest that spheroids have cell proliferation and cell differentiation.

β hCG, syncytiotrophoblast marker, was detected at spheroid cultured for 24, 48, and 72 h. The β hCG fluorescence intensity increased significantly after 24 hours and was highest in the BEWO spheroid cultured for 72 h. The β hCG relative fluorescence intensity for DAPI showed an increase, but the JAR and JEG-3 spheroid slightly decreased at 72 h, although not significant (Fig. 4). These results suggest that the spheroid of all cell lines contain syncytiotrophoblast and differentiate into syncytiotrophoblast over time.

As a result of examining the mRNA level of the genes related to implantation, β hCG was highest in BEWO spheroid cultured for 72 h, and showed a pattern similar to that of immunofluorescence result (Fig. 5A). In addition, the JEG-3 spheroid also showed mRNA level similar to the pattern of relative β hCG fluorescence intensity. However, the JAR spheroid cultured for 24h showed a higher mRNA level than other cell lines, which will require additional repetitive experiments. Syncytin-1 was expressed in all cell lines, and SYN1 is expressed in first-trimester trophoblast and expressed in choriocarcinoma cell lines (Muir et al., 2006). BEWO spheroid showed the highest mRNA level at 48 h and

maintained the high mRNA level at 72 h. JEG-3 spheroid and JAR spheroid showed the highest level at 24 h (Fig. 5C). JAR, JEG-3, and BEWO are all first-trimester trophoblast cell lines, So the spheroids already contain cells differentiated into syncytiotrophoblast. Therefore, it is presumed that the levels of β hCG and syncytin-1 mRNA do not show similar patterns. All cell lines showed high syncytin-1 mRNA levels at 24 h, and cell fusion seems to be promoted by forming a spheroid. GDF15 is a gene associated with migration and invasion in trophoblastic cells. The highest mRNA level was shown in the JAR spheroid cultured for 24 h, and no pattern was shown in other cell lines (Fig. 5B). Integrin beta3 (ITGB3) is an adhesion molecule and is known to be expressed in syncytiotrophoblast and choriocarcinoma cell lines (Natalie et al., 2010). Consistent with this, it was expressed in all cell lines and showed the highest mRNA level at the 24 h spheroid of all cell lines. At 48 and 72 h, ITGB3 mRNA levels of JAR and JEG-3 spheroid decreased, but BEWO spheroid maintained a high level (Fig. 5D). These results suggest that spheroids express genes related to implantation and have the ability to differentiate, attach and invade.

The characteristics of the spheroids were identified in the 2D co-culture system (Fig. 6). When co-cultured with AN3CA for 24 h and 48 h, the morphology of the spheroid remained unchanged, whereas when co-cultured with Ishikawa, epithelial cells around the spheroids were pushed out. In addition, the spheroids were expanded, and spheroid cells were spread out in the form of branches. This shows that the spheroids have stronger adhesion to monolayer than when co-cultured with AN3CA when co-cultured with Ishikawa. When co-cultured with Ishikawa showed an attachment rate close to 100%, but when co-cultured with AN3CA, it showed a low attachment rate. BEWO spheroid showed

a higher attachment rate when co-cultured with AN3CA than other cell line spheroid, which may be related to the high ITGB3 mRNA levels. This result suggests that spheroids can respond appropriately according to the characteristics of epithelial cells. At co-culture with Ishikawa for 48h, completely collapsed spheroids were found (fig. 7A). Both the invasion rate and area were the highest among JEG-3 spheroids. To explain these results, it is necessary to compare the expression levels of EVT markers or other invasion markers.

A 3D endometrium model was constructed, and an epithelial cell was attached to a modified PEG hydrogel using an RGD domain. This model can provide an environment similar to the invasion process by using ECM that can be degradable by MMPs. This model also may be useful for unmasking the mechanisms of human implantation. In future experiments, this will be used to observe the attachment and invasion of spheroids and to investigate the differences from the 2D culture system. In addition, the stability of the model should be analyzed by confirming whether an appropriate hormonal response is shown through decidualization induction.

REFERENCES

Aghajanova L, Hamilton AE, Giudice LC. Uterine receptivity to human embryonic implantation: histology, biomarkers, and transcriptomics. Semin Cell Dev Biol. 2008 Apr;19(2):204-11.

Aplin JD, Jones CJ, Harris LK.. Adhesion molecules in human trophoblast—a review. I. Villous trophoblast. Placenta 2009 Apr;30(4):293-8.

Ashary N, Tiwari A, Modi D. Embryo Implantation: War in Times of Love. Endocrinology. 2018 Feb 1;159(2):1188-1198.

Campbell S, Swann HR, Seif MW, Kimber SJ, Aplin JD. Cell adhesion molecules on the oocyte and preimplantation human embryo. Hum Reprod. 1995 Jun;10(6):1571-8.

Carter AM. Animal models of human placentation--a review. Placenta. 2007 Apr;28 Suppl A:S41-7.

Coughlan C, Ledger W, Wang Q, Liu F, Demirol A, Gurgan T, Cutting R, Ong K, Sallam H, Li TC. Recurrent implantation failure: definition and management. Reprod Biomed Online. 2014 Jan;28(1):14-38.

Carter AM, Enders AC, Pijnenborg R. The role of invasive trophoblast in implantation and placentation of primates. Philos Trans R Soc Lond B Biol Sci. 2015 Mar 5;370(1663):20140070.

Cook CD, Hill AS, Guo M, Stockdale L, Papps JP, Isaacson KB, Lauffenburger DA, Griffith LG. Local remodeling of synthetic extracellular matrix microenvironments by co-cultured endometrial epithelial and stromal cells enables long-term dynamic physiological function. Integr Biol (Camb). 2017 Apr 18;9(4):271-289.

Chen YH, Zhang XL, Fan JM, Li ZY, Wang J, Wang XP, Wu XQ. The possible window of implantation for embryos in the first frozen embryo transplantation cycle: A retrospective analysis. Transpl Immunol. 2022 Jun;72:101582.

Staun-Ram E, Goldman S, Gabarin D, Shalev E. Expression and importance of matrix metalloproteinase 2 and 9 (MMP-2 and -9) in human trophoblast invasion. Reprod Biol Endocrinol. 2004 Aug 4;2:59.

Evans J, Rai A, Nguyen HPT, Poh QH, Elglass K, Simpson RJ, Salamonsen LA, Greening DW. Human Endometrial Extracellular Vesicles Functionally Prepare Human Trophectoderm Model for Implantation: Understanding Bidirectional Maternal-Embryo Communication. Proteomics. 2019 Dec;19(23):e1800423.

Evans J, Walker KJ, Bilandzic M, Kinnear S, Salamonsen LA. A novel "embryo-endometrial" adhesion model can potentially predict "receptive" or "non-receptive" endometrium. J Assist Reprod Genet. 2020 Jan;37(1):5-16.

Fukui Y, Hirota Y, Matsuo M, Gebril M, Akaeda S, Hiraoka T, Osuga Y. Uterine receptivity, embryo attachment, and embryo invasion: Multistep processes in embryo implantation. Reprod Med Biol. 2019 May 24;18(3):234-240.

Fitzgerald HC, Schust DJ, Spencer TE. In vitro models of the human endometrium: evolution and application for women's health. Biol Reprod. 2021 Feb 11;104(2):282-293.

Félix Vélez NE, Gorashi RM, Aguado BA. Chemical and molecular tools to probe biological sex differences at multiple length scales. J Mater Chem B. 2022 Sep 28;10(37):7089-7098.

Governini L, Luongo FP, Haxhiu A, Piomboni P, Luddi A. Main actors behind the endometrial receptivity and successful implantation. Tissue Cell. 2021 Dec;73:101656.

Gualdoni G, Gomez Castro G, Hernández R, Barbeito C, Cebral E. Comparative matrix metalloproteinase-2 and -9 expression and activity during endotheliochorial and hemochorial trophoblastic invasiveness. Tissue Cell. 2022 Feb;74:101698.

Hannan NJ, Paiva P, Dimitriadis E, Salamonsen LA. Models for study of human embryo implantation: choice of cell lines? Biol Reprod. 2010 Feb;82(2):235-45.

Huang Q, Li J, Wang F, Oliver MT, Tipton T, Gao Y, Jiang SW. Syncytin-1 modulates placental trophoblast cell proliferation by promoting G1/S transition. Cell Signal. 2013 Apr;25(4):1027-35.

Hirota Y. Progesterone governs endometrial proliferation-differentiation switching and blastocyst implantation. Endocr J. 2019 Mar 28;66(3):199-206.

Hamutoğlu R, Bulut HE, Kaloğlu C, Önder O, Dağdeviren T, Aydemir MN, Korkmaz EM. The regulation of trophoblast invasion and decidual reaction by matrix metalloproteinase-2, metalloproteinase-7, and metalloproteinase-9 expressions in the rat endometrium. Reprod Med Biol. 2020 Aug 6;19(4):385-397.

Jason M. Franasiak, Diana Alecsandru, Eric J. Forman, Laura C. Gemmell, Jeffrey M. Goldberg, Natalia Llarena, Cheri Margolis, Joop Laven, Sam Schoenmakers, Emre Seli, A review of the pathophysiology of recurrent implantation failure, Fertility and Sterility, 2021 Dec;116(6):1436-1448.

Jensen C, Teng Y. Is It Time to Start Transitioning From 2D to 3D Cell Culture? Front Mol Biosci. 2020 Mar 6;7:33.

Joo M, Kim D, Lee MW, Lee HJ, Kim JM. GDF15 Promotes Cell Growth, Migration, and Invasion in Gastric Cancer by Inducing STAT3 Activation. Int J Mol Sci. 2023 Feb 2;24(3):2925.

Kloxin AM, Kloxin CJ, Bowman CN, Anseth KS. Mechanical properties of cellularly responsive hydrogels and their experimental determination. Adv Mater. 2010 Aug 17;22(31):3484-94.

Kim HD, Heo J, Hwang Y, Kwak SY, Park OK, Kim H, Varghese S, Hwang NS. Extracellular-matrix-based and Arg-Gly-Asp-modified photopolymerizing hydrogels for cartilage tissue engineering. Tissue Eng Part A. 2015 Feb;21(3-4):757-66.

Kim SM, Kim JS. A Review of Mechanisms of Implantation. Dev Reprod. 2017 Dec;21(4):351-359.

Kapałczyńska M, Kolenda T, Przybyła W, Zajączkowska M, Teresiak A, Filas V, Ibbs M, Bliźniak R, Łuczewski Ł, Lamperska K. 2D and 3D cell cultures - a comparison of different types of cancer cell cultures. Arch Med Sci. 2018 Jun;14(4):910-919.

Kim S, Min S, Choi YS, Jo SH, Jung JH, Han K, Kim J, An S, Ji YW, Kim YG, Cho SW. Tissue extracellular matrix hydrogels as alternatives to Matrigel for culturing gastrointestinal organoids. Nat Commun. 2022 Mar 30;13(1):1692.

Muir A, Lever AML, Moffett A. Human endogenous retrovirus-W envelope (syncytin) is expressed in both villous and extravillous trophoblast populations. J Gen Virol. 2006 Jul;87(Pt 7):2067-2071.

Miao Z, Lu Z, Wu H, Liu H, Li M, Lei D, Zheng L, Zhao J. Collagen, agarose, alginate, and Matrigel hydrogels as cell substrates for culture of chondrocytes in vitro: A comparative study. J Cell Biochem. 2018 Nov;119(10):7924-7933.

Muter J, Lynch VJ, McCoy RC, Brosens JJ. Human embryo implantation. Development. 2023 May 15;150(10):dev201507.

Nicolas P, Etoc F, Brivanlou AH. The ethics of human-embryoids model: a call for consistency. J Mol Med (Berl). 2021 Apr;99(4):569-579.

Pierro E, Minici F, Alesiani O, Miceli F, Proto C, Screpanti I, Mancuso S, Lanzone A. Stromal-epithelial interactions modulate estrogen responsiveness in normal human endometrium. Biol Reprod. 2001 Mar;64(3):831-8.

Rashid NA, Lalitkumar S, Lalitkumar PG, Gemzell-Danielsson K. Endometrial receptivity and human embryo implantation. Am J Reprod Immunol. 2011 Jul;66 Suppl 1:23-30.

Rothbauer M, Patel N, Gondola H, Siwetz M, Huppertz B, Ertl P. A comparative study of five physiological key parameters between four different human trophoblast-derived cell lines. Sci Rep. 2017 Jul 19;7(1):5892.

Staun-Ram E, Goldman S, Gabarin D, Shalev E. Expression and importance of matrix metalloproteinase 2 and 9 (MMP-2 and -9) in human trophoblast invasion. Reprod Biol Endocrinol. 2004 Aug 4;2:59.

Staun-Ram E, Shalev E. Human trophoblast function during the implantation process. Reprod Biol Endocrinol. 2005 Oct 20;3:56.

Tarrade A, Lai Kuen R, Malassiné A, Tricottet V, Blain P, Vidaud M, Evain-Brion D. Characterization of human villous and extravillous trophoblasts isolated from first trimester placenta. Lab Invest. 2001 Sep;81(9):1199-211.

Velicky P, Knöfler M, Pollheimer J. Function and control of human invasive trophoblast subtypes: Intrinsic vs. maternal control. Cell Adh Migr. 2016 Mar 3;10(1-2):154-62.

Yi H, Yang M, Tang H, Lin M. Risk Factors of Pregnancy Failure in Infertile Patients Undergoing Assisted Reproductive Technology. Int J Gen Med. 2022 Dec 30;15:8807-8817.

Zhu J. Bioactive modification of poly(ethylene glycol) hydrogels for tissue engineering. Biomaterials. 2010 Jun;31(17):4639-56.

논문개요

초기 배아 발달 동안, 착상은 포유동물의 출산률에 대한 중요한 부분입니다. 게다가, 높은 착상 실패율은 인공 생식 분야에서 여전히 주요 문제로 남아 있습니다. 그러나, 착상 실패의 메커니즘은 아직 잘 이해되지 않고 있습니다. 착상은 섬세한 배반포 조정과 배반포와 자궁내막의 대화 과정을 포함하는 복잡한 과정입니다. 인간의 착상 과정은 마우스 및 랫과 다르며, 동물 연구 결과를 인간에 적용하는 것을 제한합니다. 반면, 인간의 착상에 대한 in vivo 연구는 윤리적 문제에 의해 제약을 받습니다. 따라서, 착상 연구를 위해서는 인간과 유사한 in vitro 모델을 구축할 필요가 있습니다. 여기서, PEG 하이드로겔 및 상피 세포주 Ishikawa(수용성 자궁내막), AN3CA(비수용성 자궁내막) 및 인간 기질 세포주 T-HESC 를 사용하여 자궁내막을 모방하였고, 배반포의 경우 융모막종 세포주(예: JAR JEG-3 및 BeWo)를 사용하였습니다. 스페로이드의 크기는 배양 시간이 증가함에 따라 증가하였고, 세포 생존율은 90% 이상이었습니다. 스페로이드의 내부 구조는 세포로 가득 차 있었고, 72 시간 동안 배양된 스페로이드에서 분화된 다핵 세포 구조가 발견되었습니다. 또한, 상이한 특성의 상피 세포 단분자층에 대한 반응으로 상이한 부착 및 침윤율을 보였습니다. 이를 통해, 스페로이드는 성장하고 분화할 수 있으며, 상피 세포에 대한 적절한 반응성을 가질 수 있음을 알 수 있었다. 이를 바탕으로, 3D 배양 모델이 구축되었습니다. 종합하면, 이러한 구성된 모델은 모-배아 미세 환경을 모방하고 인간 착상에서 다양한 병태생리학적 문제를 해결하는 데 유용할 수 있음을 시사합니다.

감사의 글

먼저 석사과정을 무사히 마칠 수 있도록 깊고 높으신 학식을 바탕으로 아낌없이 지도해 주신 전용필 교수님께 감사 인사 올립니다. 그리고 논문 완성을 위해 아낌없이 조언해 주신 상명대학교 이성호 교수님과 바이오생명공학과 김다현 교수님 감사합니다.

지난 대학원 생활을 마치고 무사히 졸업할 수 있었던 것은 좋은 교수님과 연구실 동료들 덕분입니다. 2 년 동안 발생학 연구실에서 함께했던 동료들에게 감사 인사를 전합니다.

방장 보영아 항상 부족한 언니 챙겨주느라 고생 많았고, 너무 고맙다. 무사히 졸업할 수 있는 것에 너의 역할도 크다고 생각해. 정반대처럼 느껴지다가도 잘 맞는 점도 많아서 종종 힘들었던 시기에 웃으며 이겨낼 수 있었어. 가끔은 어른스러운 모습에 배울 점도 많았어. 함께 졸업하진 못했어도 너는 큰 결과와 함께 무사히 마칠 것이라 믿어 의심치 않는다. 네가 하는 모든 일을 응원할게.

좋은 동생이자 동기인 정빈아 잔잔한 것 같지만 가끔은 별난 너의 모습에 얼마나 많이 웃었는지 모르겠다. 네가 없었으면 어떻게 졸업을 했을까 싶을 정도로 고마운 게 참 많다. 너로 인해 재밌는 시간을 보낼 수 있었어. 가끔은 안 풀리는 일들도 많겠지만 너라면 잘 해낼 수 있을 거라고 믿어.

학부 동기이자 소중한 친구인 인하야 너에게 고마운 게 너무 많다. 옆에서 많은 격려와 멘탈을 잡아주고, 항상 긍정적이고 어른스러운 너의 모습이 참 멋있다고 생각했어. 너의 따듯한 마음 덕분에 얼마나 위로받았는지 모르겠다. 박사 생활뿐만 아니라 너의 앞길이 항상 빛나길 바랄게.

후배 지수와 예림, 언니들을 잘 따라주고, 장난도 유쾌하게 받아주어 고맙고 졸업준비 문제없이 잘 해내길 바란다. 힘든 일이 있을 때 도와줄 수 있는 언니가 되도록 노력할게. 그리고 오랜 학부 생활이 쉽지 않았을 텐데 열심히 해주었던 주희와 희지에게 고맙고, 곧 시작되는 대학원 생활에 행운이 깃들길 바란다.

너희와 함께 할 수 있었던 것은 큰 행운인 것 같아. 사말싶!

마지막으로 항상 사랑과 응원을 아끼지 않고 딸내미를 지지해 준 아버지와 어머니에게 감사드립니다. 아프고 힘든 시간이 길었지만 앞으로는 부모님의 앞길에 행복이 가득하면 좋겠습니다. 평소에 무뚝뚝한 딸이지만 마음속으로는 많이 사랑하고 있습니다. 더 자랑스러운 딸이 되도록 노력할게요.

그 밖에도 말씀드리지 못한 모든 분들께 감사하며, 부족한 글 솜씨지만 모두에게 마음이 전해졌길 바랍니다.

2023 년 12 월

김지선